of the absorption profile of $1s^2$-$1s3p$ indicates a density of about $(6-7)\times10^{23}$ cm^{-3}. Hydrodynamic simulations predict a figure closer to 9×10^{23} cm^{-3}. More detailed analysis of such spectra offers the possibility of future direct comparisons between spectra and radio chemistry[8] diagnostics.

The laser-driven implosions were simulated in one dimension with the Lagrangian hydrodynamics code LASNEX.[9] The laser temporal profile used in the calculations is an accurate replica of measurements made with fast pyroelectric detectors and a 5-GHz-bandwidth oscilloscope. The hot-electron temperature is constrained to be equal to the value obtained from fast-ion measurements.[10] A particularly fine zoning (of the Lagrangian grid) is used in the outer laser absorption region. In Table I, we show comparisons of experiment and theory for several important implosion parameters.

In conclusion, CO_2-laser-driven implosions have been shown to yield high densities under conditions which also produced significant thermonuclear yield. The highest total mass densities reached in these experiments was 2–3 g/cm^3. With respect to inertial confinement fusion, these experiments have shown that the highly efficient CO_2-laser driver (~2 overall laser efficiency) is capable of producing high-density implosions.

We would like to acknowledge many helpful discussions with Professor C. F. Hooper. We would like to thank the Los Alamos Scientific Laboratory target fabrication group for production of the targets used in this study. This work was performed under the auspices of the U. S. Department of Energy.

[1]B. Yaakobi, D. Steel, E. Thorsos, A. Hauer, and B. Perry, Phys. Rev. Lett. 39, 1526 (1977).

[2]K. Mitchell, D. van Hulsteyn, G. McCall, P. Lee, and H. Griem, Phys. Rev. Lett. 42, 232 (1979).

[3]B. Yaakobi, S. Skupsksy, R. L. McCrory, C. F. Hooper, H. Deckman, P. Bourke, and J. Soures, Phys. Rev. Lett. 44, 1072 (1980); P. Auerbach *et al.*, Phys. Rev. Lett. 44, 1672 (1980).

[4]A. Hauer, Los Alamos Scientific Laboratory Report No. LA-UR-80-1660, 1980 (unpublished). See also Proceedings of the Fifth International Conference on Spectral Line Shapes, West Berlin, Federal Republic of Germany, November 1979 (to be published).

[5]P. C. Kepple and H. R. Griem, Naval Research Laboratory Memorandum No. 3634 (1978) (unpublished); H. R. Griem, M. Blaha, and P. C. Kepple, Phys. Rev. A 19, 2421 (1979).

[6]P. C. Kepple and J. Rogerson, Naval Research Laboratory Memorandum No. 4216 (1980) (unpublished).

[7]M. M. Mueller, Bull. Am. Phys. Soc. 24, 1053 (1979), and Los Alamos Scientific Laboratory Report No. LA-UR-78-2698, 1978 (unpublished) (available from Mueller).

[8]F. Mayer and W. R. Rensel, KMS Fusion, Ann Arbor, Michigan Report No. U422, 1973 (unpublished).

[9]G. Zimmerman and W. Kruer, Comments Plasma Phys. 2, 85 (1975).

[10]T. H. Tan and G. H. McCall, Los Alamos Scientific Laboratory Report No. LA-UR-80-900, 1980 (to be published).

V-Shaped Double Layers Formed by Ion Beam Reflection

R. L. Stenzel,[a] M. Ooyama, and Y. Nakamura

Institute of Space and Aeronautical Science, University of Tokyo, Komaba, Meguro-ku, Tokyo 153, Japan

(Received 20 June 1980)

A potential double layer is observed when an ion beam is injected into a collisionless magnetoplasma along converging magnetic field lines and reflected at a positive electron-absorbing boundary. The double layer is *V* shaped, highly stationary, strong ($e\varphi/kT_e \lesssim 25$) with amplitude determined by the beam energy ($\varphi \gtrsim V_b$), and occurs with magnetized (H_2^+) and unmagnetized (Ar^+) ions. Distribution function measurements show self-consistently formed trapped electrons on the high-potential side.

PACS numbers: 52.35.Mw, 52.40.Kh, 94.30.Kq

Potential double layers are of general interest in nonlinear plasma physics and of particular interest in space plasmas where they are thought to be the source for energetic auroral particles.[1] Double layers have been produced in the laboratory by various methods such as ionization processes in current-carrying discharge tubes[2,3] or injection of drifting electron distributions from cathodes[4] and plasma sources.[5-7] Because of relevance to space plasmas the recent interest has

shifted to double layers in magnetized ionization-free plasmas. In this Letter we report the observation of strong double layers in a laboratory plasma with magnetized ions. A new mechanism for generating double layers by means of reflected ion beams is described. Distribution functions differing from the standard pairs of trapped and free particles are observed.

The experiment is performed in a double-plasma device with surface magnetic field confinement in a parameter range $n_e \simeq 10^8$ cm^{-3}, $T_e \simeq 2$ eV, $p \simeq 7\times 10^{-5}$ Torr H_2 and 2×10^{-5} Torr Ar. As shown in Fig. 1 an ion beam is generated by a source plasma and injected against a permanent magnet (6 cm diameter, 2 cm length, $B \simeq 500$ G at pole face) located in the center of the target plasma. A weak uniform axial magnetic field ($B_0 \simeq 20$ G) generated by external Helmholtz coils is superimposed in the direction opposite to the axial magnetic dipole. Thus, within the separatrix (dashed curve) all field lines are closed via the magnet while outside there are open field lines. Both pole faces of the magnet form two electrically insulated electrodes which can be biased separately. The diagnostics includes axially and radially movable emissive probes, ion velocity analyzers, and Langmuir probes.

When the magnet surfaces are biased positive so as to draw electron saturation current an electron-rich sheath of a few Debye lengths ($\lambda_D = 0.83$ mm) is formed as shown in Fig. 2(a). A field-aligned electron current ($I \simeq 1$ mA) is drawn whose density increases toward the magnet because of current and magnetic flux conservation. At the magnet surface the current density is measured ($j_{e\max} = 0.14$ mA/cm^2, radial half width $\Delta r \simeq 1.5$ cm) which corresponds to a drift below the electron thermal speed in the plasma up to the sheath edge. Now an ion beam of energy eV_b is injected in the direction of the electron drift and reflected at the front magnet surface of potential $V_m > V_b > kT_e/e$. Potential profile and collected current are free to evolve. As shown in Fig. 2(a) we observe the formation of a stable double layer of width $L \simeq 14\lambda_D$ and potential height $\varphi \simeq 8.8kT_e/e \lesssim V_b$ well separated from the narrow sheath ($< 5\lambda_D$) of residual potential drop $V_m - \varphi$. No double layer is formed unless $V_m \gtrsim V_b$. Within this constraint double layers are observed in a wide parameter range ($3 \lesssim e\varphi/kT_e \lesssim 25$) with nearly predictable amplitudes [see Fig. 2(b)]. From the slope of the potential profile ($\partial\varphi/\partial z \simeq 13$ V/cm) and the temporal fluctuations ($\delta\varphi \simeq 1$ V_{rms}) we find the layer to be stationary to within $\delta z \simeq 0.8$ mm ($\approx \lambda_D$!). Differentiating $\varphi(z)$, we obtain from Poisson's law a net charge density $n_{\max} = 1.2\times 10^7$ cm^{-3} of ions on the high-potential side, the same number of excess electrons on the low-potential side, at a target-plasma density $n_{e0} \simeq 1.4\times 10^8$ cm^{-3}. In the presence of the double layer, the collected electron current to the front surface ($I_m \simeq 5$ mA) is ~5 times larger than to the back side at the same bias.

Figure 3 shows the magnetic field topology and two-dimensional potential contours for light ions. Beam analysis by time of flight indicates that in hydrogen the dominant ion species is H_2^+. The decelerated hydrogen beam ions ($kT_\perp \ll \frac{1}{2}mv_\parallel^2 \ll eV_b$) and the background ions ($kT_i \simeq 0.2$ eV) are reasonably magnetized near the double layer or closer toward the magnet ($r_{ci} = 7$ mm at $B = 200$ G, $kT_\perp = 0.5$ eV). In contrast, the Ar^+ Larmor radius is comparable to the magnet dimensions. The contours of constant plasma potential φ_p in H_2^+ [Fig. 3(b)] are V shaped indicating a maximum

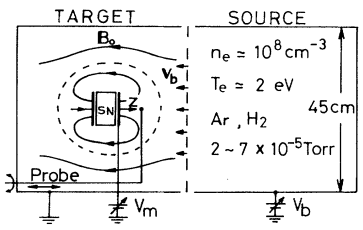

FIG. 1. Schematic view of the experimental setup.

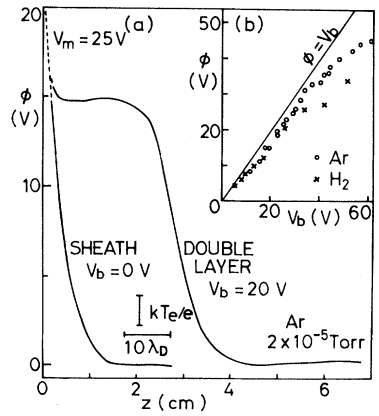

FIG. 2. (a) Potential φ (relative to target plasma potential) vs distance z from magnet biased at V_m. A double layer is formed in the presence of a reflected ion beam of energy $eV_b < eV_m$. (Argon, $kT_e = 1.7$ eV, $n_{e0} = 1.3\times 10^8$ cm^{-3}). (b) Double-layer potential jump vs beam voltage in argon and H_2 ($kT_e = 2.8$ eV in H_2).

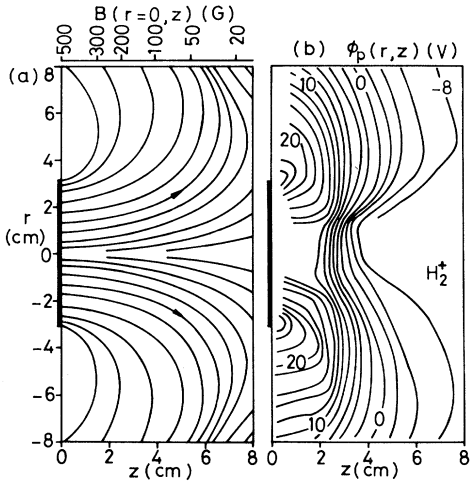

FIG. 3. (a) Magnetic field lines (arbitrarily spaced) and axial field strength (top scale) in front of magnet surface (indicated by heavy line) ($B=0$ at $r=0$, $z=10.5$ cm). (b) Contours of constant plasma potential ($\Delta\varphi_p=2$ V between contours) showing a V-shaped double layer in H_2 ($V_b=30$ V, $V_m=38$ V).

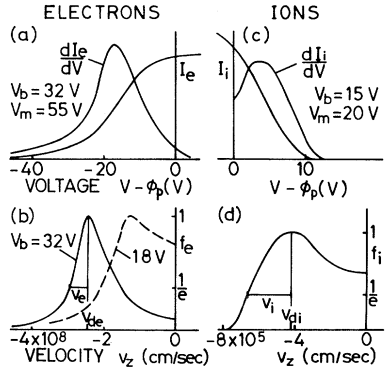

FIG. 4. Distribution functions on the high-potential side of the double layer ($r=0$, $z=0.5$ cm) for velocities toward the magnet (argon, 2×10^{-5} Torr). (a), (c) Original collector I-V curves and graphically formed derivatives for electrons and ions, respectively. (b) Electron velocity distribution for $V_b=32$ V ($\frac{1}{2}mv_e^2=0.85$ eV $<kT_{e0}=1.7$ eV, $\frac{1}{2}mv_{de}^2=18$ eV $<e\varphi_p\simeq 21$ eV) and for $V_b=18$ V (dashed line) where asymmetric distribution is more pronounced. (d) Ion velocity distribution ($\frac{1}{2}mv_{di}^2\simeq 3.6$ eV, $\frac{1}{2}mv_i^2\simeq 1.2$ eV).

parallel field $E_\parallel\simeq 10$ V/cm at $z\simeq 3$ cm limited radially to the central current-carrying channel. $E_\parallel$ and $E_\perp$ are of comparable magnitude. Strong positive-potential islands arise near the magnet's periphery where $B\simeq 1000$ G and $n_e\to 0$ because of small cross-field diffusion but $n_i>0$ because of beam injection with $r_{ci}\gg r_{ce}$. Without ion beam or $V_m<V_b$ the potential contours outside the sheath are field aligned. In Ar^+ the radial extent of the double layer with $\vec{E}\parallel\vec{B}$ is wider than in H_2^+, i.e., the double layer is more plane than V shaped. Nevertheless, at large r the curvature of $\vec{B}$ implies $\vec{E}_z\perp\vec{B}$.

A small (4 mm diameter) retarding grid velocity analyzer has been used to measure distribution functions. With the analyzer in front of the magnet ($r=0$, $z=5$ mm) and its outer grid biased to the magnet potential (which does not perturb the potential profile as verified by the emissive probe) the electron distribution is obtained from the collector I-V characteristic. Figure 4 shows $f_e(v_z)$ for $v_z<0$ at two different beam voltages in Ar^+. In contrast to all previous experiments on double layers we have no electron source on the high-potential side which provides for trapped electrons. Ionization cannot be significant since the double layers are also observed in an afterglow plasma and at potential levels below the ionization potential. Thus, the slow electrons observed must be produced self-consistently from the free electron population by mirror reflection, wave-particle scattering to reduce the parallel velocity, and electrostatic reflection by the double layer. These scattering processes require an interaction length which increases with velocity. At high potentials ($V_b=32$ V, $\varphi_p\simeq 21$ V) we observe almost only free accelerated electrons with $v_{de}/v_e\simeq 5$. This distribution is subject to the classic Buneman instability.[8] The observed fluctuation spectrum is broad ($\omega_{max}\simeq 2\pi\times 4$ MHz $\gg\omega_{pi}$ in Ar). A detailed analysis of the turbulence will be published later. At lower drift speeds ($V_b=18$ V, $v_{de}/v_e\simeq 1.6$) the number of slow electrons increases dramatically as evident from the asymmetry of the shifted distribution. From measurements of the distribution function, the radial current density profile and the total current to the magnet we determine the electron density at the analyzer's position to be $n_e=1.25\times10^8$ cm^{-3} at $V_b=18$ V (0.66×10^8 cm^{-3} at 32 V).

Using the velocity analyzer for ions, we observe at the low-potential side or for $V_m=0$ the incident ion beam and the low-energy background ions, both with comparable fluxes. At the high-potential side of the double layer ($r=0$, $z=5$ mm) only one ion population is seen with considerable energy spread around the local plasma potential. These are the retarded beam ions since all low-energy ions are reflected at the double layer. Independently, the retardation of beam ions has

been established by small-amplitude sinusoidal beam density modulation and dispersion measurements $\omega \simeq kv_b$. At the double layer the phase velocity decreases rapidly and the amplitude vanishes without reflections. No ion acoustic waves could be excited on the high-potential side, presumably because $T_i \gtrsim T_e$. Although not directly measured the ion distribution for $v_z > 0$ must contain the reflected ions since none are absorbed by the magnet.

The evolution of the double layer has been studied by pulsing V_m or V_b. The sheath potential expands, changes curvature to form an inflection point, i.e., a weak double layer, which propagates into the plasma at decreasing velocity ($v < C_s$) but growing in amplitude and gradient. The buildup time is approximately 50 μsec (in argon) whereas the decay after turnoff of V_m is within $\tau \lesssim 5$ μsec. The switching process is accompanied by large waves and particle bursts.

These observations lead to the following simplified physical picture for the double layer formation: Beam ions enter the electron-rich sheath, decelerate to rest and form a positive-space-charge layer ($n_i > n_e$). The potential profile expands so that acceleration of electrons, retardation of beam ions and reflection of background ions occur at increasing distances from the magnet. Experimentally we find that the final position and potential jump of the double layer adjust themselves so as to establish charge neutrality on the high-potential side. With rising potential the retarded-ion-beam density increases $[n_i = n_b(1 - \varphi/V_b)^{-1/2}]$ while the accelerated-electron density decreases $[n_e = n_{e0}(1 + e\varphi/kT_e)^{-1/2}]$. Since at the low-potential side the ratio of beam to electron density is small $\{n_b/n_{e0} < [1 + (2\, eV_b/kT_e)^{1/2}]^{-1}\}$ the potential must adjust itself close to $\varphi \lesssim V_b$ in order to satisfy $n_i = n_e$. This is even more required when trapped electrons increase n_e which is pronounced at low V_b [see Fig. 4(b)] consistent with the shape of Fig. 2(b). The position of the double layer approaches a stationary value because of the axial-magnetic-field dependence. With increasing distance from the magnet the double-layer area increases ($S \propto B^{-1}$) implying increased electron density toward the magnet since the electron current and not the flux is conserved ($I_m = Sn_e ev = \text{const}$). The position is found to increase when, at a given V_b, the collected current I_m is increased by raising V_m, thus the position regulates the electron supply. Likewise, when the ion density is raised by a larger source-plasma density the double-layer position increases so as to establish charge neutrality self-consistently. In this manner the double layer can be positioned anywhere between $0 \lesssim z \lesssim 8$ cm. Finally, $V_m > V_b$ is an essential requirement to generate the return ion flow through the double layer. Magnetized ions with finite $v_\perp$ undergoing parallel deceleration by the mirror magnetic field can also be reflected at the double layer when $\varphi < V_b$. At their stagnation point near the high-potential side, they contribute to the positive-space-charge layer.

In summary, we have observed a new mechanism for generating double layers in a magnetoplasma. From the laboratory observations, we speculate on the following scenario in space: Given a distributed potential difference between a highly conducting boundary such as the ionosphere and the distant magnetosphere, the potential profile can steepen into a V-shaped double layer when energetic ions from the magnetotail precipitate down along a dipolar flux tube, stagnate and reflect at a location where $e\varphi = \frac{1}{2}mv_\parallel{}^2$, and form a positive-space-charge layer. Such Earthward streaming protons are thought to be an energy source of precipitating electrons responsible for auroras.[9] The double-layer potential is determined by the ion energy. Reconnection processes may be the origin for energetic ion precipitation while the potential difference is set up by the solar-wind dynamo action.

The expert technical help from Mr. Y. Nomura is greatly appreciated. One of the authors (R.L.S.) acknowledges support from the Institute of Space and Aeronautical Science.

---

[a]On sabbatical leave from Department of Physics, University of California, Los Angeles, Cal. 90024.

[1]H. Alfvén and P. Carlquist, Sol. Phys. 1, 220 (1967); L. P. Block, Cosmic Electrodyn. 3, 349 (1972); F. S. Mozer *et al.*, Phys. Rev. Lett. 38, 292 (1977).

[2]I. Langmuir, Phys. Rev. 33, 954 (1929).

[3]S. Torvén and D. Anderson, J. Phys. D 12, 717 (1979).

[4]S. Iizuka, K. Saeki, N. Sato, and Y. Hatta, Phys. Rev. Lett. 43, 1404 (1979).

[5]B. H. Quon and A. Y. Wong, Phys. Rev. Lett. 37, 1393 (1976).

[6]P. Coakley and N. Hershkowitz, Phys. Fluids 22, 1171 (1979).

[7]K. D. Baker, L. P. Block, R. Kist, and W. Kampa, Proc. Int. Conf. Plasma Phys. 1, 417 (1980).

[8]O. Buneman, Phys. Rev. 115, 503 (1959).

[9]D. W. Swift, Space Sci. Rev. 22, 35 (1978).